Dynamic Droplet Modulation

DOI: 10.1002/anie.200603072

Dynamic Modulation of Chemical Concentration in an Aqueous Droplet**

*Gavin D. M. Jeffries, Jason S. Kuo, and Daniel T. Chiu**

Chemical and biological processes are governed by the frequency of molecular collisions, which are dictated by the concentration of the dissolved species. The activities and assembly of proteins confined within cellular and subcellular compartments, for example, can be modulated by their concentrations owing to effects of macromolecular crowding.[1] To control the reactivity of single molecules and ultrasmall samples,[2–5] droplets have recently emerged as an attractive platform.[3–10] Herein we describe the use of a Laguerre–Gaussian (LG) beam to generate an optical vortex trap,[11,12] which then dynamically alters the concentration of the dissolved species within individual aqueous droplets while simultaneously allowing translational control. These aqueous droplets, which have volumes in the femtoliter (10^{-15} L) range, are surrounded by an immiscible continuous phase with a slight solubility for water, but the aqueous–organic interface is impenetrable to the encapsulated chemical species.

Figure 1a illustrates our scheme for vortex trapping of aqueous droplets in which the TEM_{00} output of an Nd:YAG laser (1064 nm) was shaped into a LG_0^1 beam (magnification on the right) by using a hologram; subsequent focusing of the LG_0^1 beam generates the requisite vortex trap for the manipulation of aqueous droplets. As water usually has a lower refractive index than the immiscible medium, conventional optical tweezers cannot be applied to the direct trapping and manipulation of aqueous droplets. In fact, optical tweezers will displace rather than trap the droplet because the trap becomes a point of instability for low-refractive-index particles. In contrast, the ring of laser intensity that surrounds the dark core of a vortex trap effectively acts as a light cage for the manipulation of the light-confined droplet (see circled magnification on the left in Figure 1a). Figure 1b–e shows a sequence of images showing the trapping and translation of an approximately 5 fL aqueous droplet dispersed in acetophenone. This approach has advantages over other droplet manipulation techniques as it is easy to implement into complex chip designs, is applicable to small, individually selected droplets, and works dynamically on the droplet of interest.

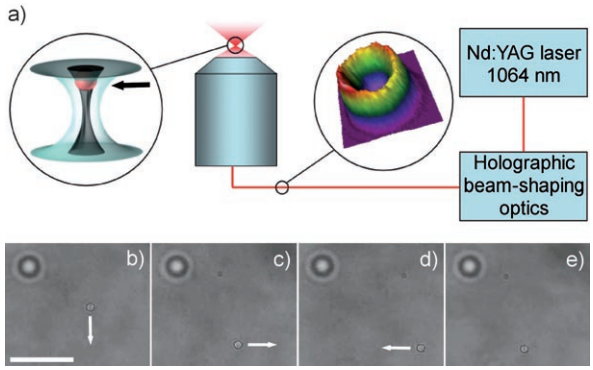

Figure 1. a) The output of the Nd:YAG laser at 1064 nm was focused through a microfabricated hologram to form the LG beams. The desired LG mode was then selected, spatially filtered, and used for vortex trapping. The arrow indicates the trapping position of a droplet in the vortex trap. b–e) A sequence of images that depict the vortex trapping and translation of an approximately 2 μm aqueous droplet (in focus) near the center of the image. The arrow denotes the direction of translation of the vortex trap, which is illustrated by using the surface bound droplet in the top left corner as a reference (out of focus). The scale bar in panel (b) represents 10 μm.

Figure 2 shows our experimental findings in which the optical vortex trap slowly "peeled off" layers of water molecules at the interface of the aqueous and immiscible fluids (Figure 2a–c, f–h), thus concentrating the encapsulated molecules that were retained within the droplet.[3] When the power of the vortex trap was lowered or turned off, the water molecules that had left the droplet returned to the droplet (Figure 2c–e, h–j), thereby leading to a volumetric expansion of the droplet. To prevent passive diffusion of water from the droplet into the immiscible phase, the immiscible phase was presaturated with water in these experiments.[3]

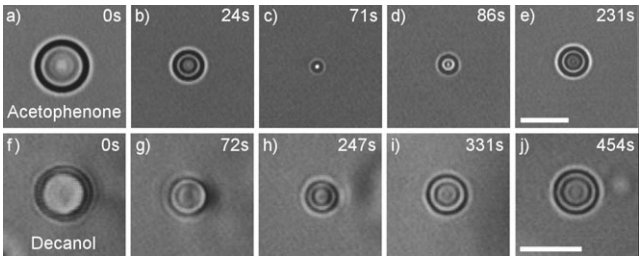

Figure 2. Shrinkage and expansion of aqueous droplets dispersed in acetophenone (a–e) and decanol (f–j); the scale bar in panels (e) and (j) represents 5 μm. To stabilize the droplets, we used a nonionic surfactant Span 80 (0.1%wt) in both the acetophenone and the decanol immiscible phases. The laser power used was approximately 43 mW, which was measured as the beam exited the objective.

[*] G. D. M. Jeffries, Dr. J. S. Kuo, Prof. D. T. Chiu
Department of Chemistry
University of Washington
Box 351700, Seattle, WA 98195-1700 (USA)
Fax: (+1) 206-685-8665
E-mail: chiu@chem.washington.edu

[**] Support for this work from the NSF (CHE-0135109) and the NIH (GM 65293) is gratefully acknowledged.

The dominant mechanism that underlies this droplet shrinkage is the localized heating (≤ 1 K) of the interface in which the droplet and vortex beam overlap. This results in a localized solubility increase of water in the organic phase that immediately surrounds the trapped droplet. Through the use of a temperature rise of 1 K, the increase in solubility was calculated to be 6.0×10^{-3} moles L^{-1}, which leads to a rate of mass loss of approximately 8.8×10^{-12} g s^{-1} at the interface of a 5-μm droplet. When the power of the vortex trap is decreased or turned off, the water that is dissolved in the surrounding oil phase returns to the droplet, thus leading to droplet expansion. The degree to which the droplet can expand back to its original size prior to shrinkage therefore depends on the ability of the dissolved water to return to the droplet after shrinkage.

Figure 3 a–g shows three sequential cycles of shrinkage and expansion. Additionally, it is possible to expand the volume of one droplet beyond its original size by accumulating the water released during the shrinkage of an adjacent droplet. Figure 3 h–k shows the shrinkage of a "donor" droplet confined in a microfluidic chamber, which caused a fivefold increase in the volume of an adjacent "target" droplet.

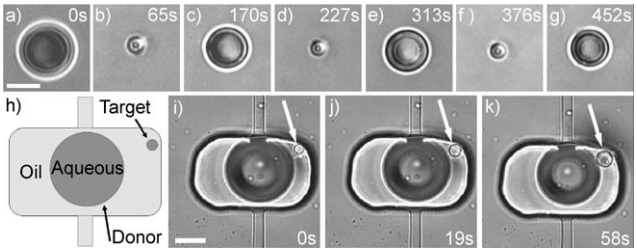

Figure 3. a–g) A sequence of images showing three consecutive cycles of droplet shrinkage and expansion in acetophenone with Span 80 (0.1 %) as a surfactant. The scale bar in (a) represents 5 μm. h) A diagram illustrating the arrangement of two droplets in a microfluidic chamber. i–k) A sequence of images showing the expansion in volume (≈5 times) of a target droplet (indicated by the arrow) caused by the optically induced shrinkage of the nearby "donor" droplet. The scale bar in (i) represents 10 μm.

To verify that the shrinkage is indeed owing to absorption of laser radiation, we systematically varied the trapping powers as well as replaced H_2O with D_2O (Figure 4). We observed that the shrinkage rates for D_2O were significantly lower than the shrinkage rates in experiments in which H_2O was used as the aqueous phase (Figure 4 a).

The initial rate of shrinkage of a D_2O droplet was (18 ± 4) % of the rate for H_2O droplets. The difference is consistent with the lower absorption cross section (≈15 %) of D_2O in comparison with H_2O at 1064 nm (Figure 4 b). We numerically modeled, with a moving boundary condition to account for droplet shrinkage, the heat- and mass-transfer phenomenon in our experiments.[13,14] By using this model, we determined the temperature increase within the droplet to be less than 1 K under our experimental conditions owing to rapid thermal conduction at this high surface-to-volume ratio. Our model agreed quantitatively with our experimental data

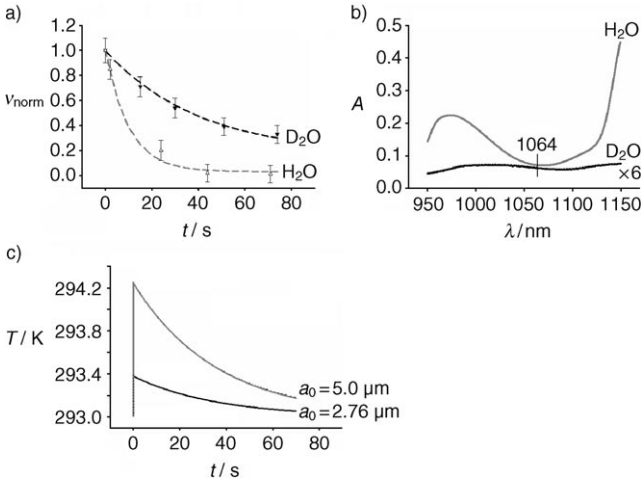

Figure 4. a) Plots of experimentally measured shrinkage rates for H_2O and D_2O droplets in acetophenone. The initial volumes of the droplets were normalized so their respective rates can be compared. b) Absorption spectra of H_2O and D_2O showing the difference in absorption at 1064 nm. Note the values in the D_2O spectrum have been multiplied by six times to ease visualization and comparison. c) Simulated temperature change of H_2O droplets during shrinkage in a vortex trap. Initial laser absorption causes a sharp rise in droplet temperature, however, this rise is limited to approximately 1.3 K for a 5-μm-radius droplet. As time progresses, the droplet temperature decreases because of the increase in the surface-to-volume ratio of the shrinking droplet. The two traces correspond to droplets with initial radii (a_0) of 5.0 μm and 2.76 μm. V_{norm} = normalized volume.

and accounted for the differences in the shrinkage rate between D_2O and H_2O droplets. The calculated temperature rise of a 5-μm-radius H_2O droplet in acetophenone was approximately 1.3 K under our experimental conditions, which is also consistent with the typical literature values of temperature rise in H_2O caused by heating from a conventional optical tweezer.[15,16] Figure 4 c shows the calculated temperature change in droplets of two different initial sizes. As the droplet shrank, the surface-to-volume ratio increased, resulting in enhanced heat transfer. Similarly, there is less temperature rise in small droplets than large droplets because of more efficient thermal conduction away from the small droplet. We attempted to verify the temperature rise experimentally by using rhodamine B (a temperature-sensitive fluorescent dye) to measure the temperature change during droplet shrinkage.[17] This method is capable of detecting temperature variations of approximately 2 K under well-calibrated conditions, however, we found that this sensitivity was insufficient for discerning any temperature change in the vortex-trapped droplet. Hence, we experimentally verified the temperature rise to be approximately less than 2 K.

Finally, we applied this phenomenon to modulate dynamically the concentration of dissolved species contained within an aqueous droplet. Figure 5 a shows one cycle of concentration and dilution of Alexa 488 dye molecules, again illustrating the reversibility and tunability of this phenomenon in controlling chemical concentrations. As the diameter of the droplet decreased, its z position changed and became trapped closer to the laser focus;[18] the inverse occurred as the

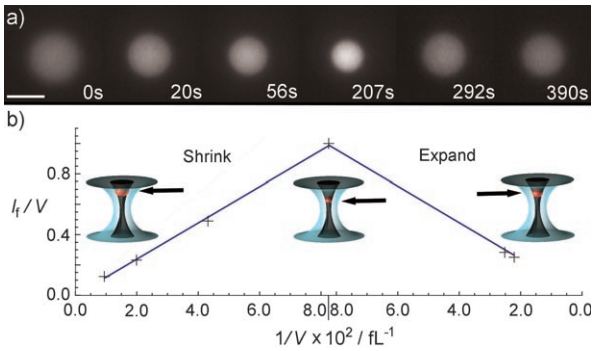

Figure 5. a) Fluorescence images of an aqueous droplet containing Alexa 488 (≈100 μM) as the droplet went through one cycle of shrinkage and expansion in acetophenone. Fluorescence imaging was performed with the line at 488 nm of an Ar^+ ion laser and a charge-coupled device (CCD) camera. The scale bar to the left of the panel represents 3 μm. b) Plot of normalized fluorescent intensity per unit volume versus the respective reciprocal volume. The plot depicts species conservation; the insets illustrate the change in the trapping position of the droplet (indicated with an arrow) in the axial direction as the droplet changes in volume. I_f = fluorescence intensity.

droplet expanded in size (see pictures in Figure 5b, where the trapping position is indicated with an arrow).

The position of the droplet in the vortex trap is largely governed by the gradient force; as the droplet shrinks, its position along the optical axis must shift to remain at the lowest potential. The magnitude of the two slopes in the plot of fluorescence intensity versus the reciprocal volume is identical (Figure 5b). This indicates that the dissolved Alexa dyes were completely retained within the droplet as its volume shrank and expanded.[3]

By using a vortex trap, we were able to concentrate species by over four orders of magnitude without effecting any noticeable temperature changes in the system. Dynamic control over the concentrations of dissolved species in a nanoscale reaction vessel provides a new degree of control that was previously difficult to achieve in a macroscopic chemical system. By combining this technique with controlled single-droplet fusion, we believe this phenomenon will find use in the study of fundamental chemical processes ranging from effects of macromolecular crowding to protein nucleation and crystallization.

Experimental Section

Preparation of aqueous droplets: To produce the aqueous droplets, we made emulsions by mixing a 10:1 volumetric ratio of continuous organic phase (e.g. acetophenone) and dispersed aqueous phase. Surfactant (Span 80; 0.1% wt) was added to the continuous phase to aid in the dispersion and to increase the stability of the droplets by minimizing droplet flocculation and fusion. This approach yielded aqueous droplets of various diameters. The emulsion was allowed to stand, which led it to the beginning of phase separation. This process caused a crude fractionation of the droplets by size so that we could extract droplets from a volume fraction that contained the desired droplet sizes. The organic phase we used was presaturated with water; the phase-segregated oil and aqueous solutions were periodically agitated over the course of three days. All chemicals were purchased from Sigma Aldrich (Milwaukee, WI, USA).

Fabrication of the hologram: To generate the LG beams, we used a transmissive phase hologram. To microfabricate this hologram, first we had to generate a binary mask to be used in photolithography. This photomask was created by calculating the interference pattern between a TEM_{00} and a LG_0^1 beam and the calculated pattern was then written onto a chrome blank. The transmissive hologram was fabricated in SU8 (Microchem, Newton, MA, USA) by using standard procedures in photolithography and SU8 processing.[4,5] Briefly, we spin-coated a thin layer (≈65 μm) of SU8 onto a number 1 glass coverslip. The SU8 was prebaked, UV exposed under the photomask, then postbaked and developed according to standard procedures.[4,5]

Received: July 29, 2006
Revised: November 17, 2006
Published online: January 4, 2007

Keywords: laser chemistry · nanotechnology · reaction control · vortex trapping

[1] A. P. Minton, *Biophys. J.* **2005**, *88*, 971.
[2] D. T. Chiu, C. F. Wilson, F. Ryttsen, A. Stromberg, C. Farre, A. Karlsson, S. Nordholm, A. Gaggar, B. P. Modi, A. Moscho, R. A. Garza-Lopez, O. Orwar, R. N. Zare, *Science* **1999**, *283*, 1892.
[3] M. He, C. Sun, D. T. Chiu, *Anal. Chem.* **2004**, *76*, 1222.
[4] M. He, J. S. Edgar, G. D. M. Jeffries, R. M. Lorenz, J. P. Shelby, D. T. Chiu, *Anal. Chem.* **2005**, *77*, 1539.
[5] R. M. Lorenz, J. S. Edgar, G. D. M. Jeffries, D. T. Chiu, *Anal. Chem.* **2006**, *78*, 6433.
[6] B. Zheng, C. J. Gerdts, R. F. Ismagilov, *Curr. Opin. Struct. Biol.* **2005**, *15*, 548.
[7] B. Zheng, J. D. Tice, R. F. Ismagilov, *Anal. Chem.* **2004**, *76*, 4977.
[8] C. X. Luo, X. J. Yang, O. Fu, M. H. Sun, Q. Ouyang, Y. Chen, H. Ji, *Electrophoresis* **2006**, *27*, 1977.
[9] A. R. Wheeler, H. Moon, C.-J. Kim, J. A. Loo, R. L. Garrell, *Anal. Chem.* **2004**, *76*, 4833.
[10] K. T. Kotz, Y. Gu, G. W. Faris, *J. Am. Chem. Soc.* **2005**, *127*, 5736.
[11] D. G. Grier, *Nature* **2003**, *424*, 810.
[12] N. B. Simpson, D. McGloin, K. Dholakia, L. Allen, M. J. Padgett, *J. Mod. Opt.* **1998**, *45*, 1943.
[13] R. L. Armstrong, *Appl. Opt.* **1984**, *23*, 148.
[14] F. M. Kuni, E. A. Grinina, A. K. Shchekin, *Colloid J.* **2003**, *65*, 740.
[15] Y. Liu, D. K. Cheng, G. J. Sonek, M. W. Berns, C. F. Chapman, B. J. Tromberg, *Biophys. J.* **1995**, *68*, 2137.
[16] E. J. G. Peterman, F. Gittes, C. F. Schmidt, *Biophys. J.* **2003**, *84*, 1308.
[17] D. Ross, M. Gaitan, L. E. Locascio, *Anal. Chem.* **2001**, *73*, 4117.
[18] K. T. Gahagan, G. A. Swartzlander, Jr., *J. Opt. Soc. Am. B* **1998**, *15*, 524.

